

Effect of 1-Acetyl-1H-Benzotriazole on Corrosion of Mild Steel in 1M HCl

P. P. Kamble*, R. S. Dubey

Department of Chemistry, R. J. College of Arts, Science and Commerce, University of Mumbai, Ghatkopar (W), Mumbai-400086, India

Received 29 March 2021, accepted in final revised form 19 July 2021

Abstract

The corrosion inhibition study of 1-acetyl-1H-benzotriazole (ABTZ) on mild steel in 1M HCl solution has been investigated using different techniques like weight loss, open circuit potential (OCP), and potentiodynamic polarization. Results showed that ABTZ inhibited mild steel corrosion in acid solution and indicated that the inhibition efficiencies increased with the increase in inhibitor concentration. The polarization curves revealed that the studied compound behaved as a mixed-type of inhibitor. The adsorption of the inhibitor on the surface of mild steel in the corrosive environment followed the Langmuir isotherm. The presence of thin film formed due to adsorption of ABTZ on mild steel surface is further confirmed by scanning electron microscopy (SEM) and energy dispersive X-ray analysis (EDAX).

Keywords: Mild steel; Triazole; HCl; SEM/EDAX.

© 2021 JSR Publications. ISSN: 2070-0237 (Print); 2070-0245 (Online). All rights reserved.
doi: <http://dx.doi.org/10.3329/jsr.v13i3.52725>

J. Sci. Res. **13** (3), 979-988 (2021)

1. Introduction

Mild steel is the most common choice of material used extensively in the production and transportation of crude oil in the oil and natural gas industry [1]. The main problem concerning mild steel application is its relatively low corrosion resistance in acidic solutions [2]. Hydrochloric acid solutions are widely used for acid cleaning, industry acid pickling, oil well acidizing, and acid descaling [3]. The strong acid medium can cause structural damage to mild steel. Therefore, the use of inhibitors is one of the most practical method for protecting metal against corrosion in acid media [4]. A variety of organic compounds act as corrosion inhibitors for mild steel during the acidizing procedure in the presence of HCl. Organic compounds containing a heteroatom such as nitrogen, sulfur, phosphorous, oxygen, aromatic ring, heterocyclic ring, double bond, and triple bond in their structures serve as suitable corrosion inhibitors of metals with great effectiveness in the aggressive acidic environment [5-8]. The inhibition efficiency of compounds attributed by different heteroatom is O<N<S<P. Compounds containing more than one heteroatoms like nitrogen and oxygen in their structure serves as excellent corrosion inhibitor than those containing nitrogen and oxygen alone [9,10].

*Corresponding author: pratapkamblerjc@gmail.com

In the present investigation, an attempt has been made to study the inhibitive effects of 1-acetyl-1H-benzotriazole on corrosion of mild steel in 1M HCl using weight loss and electrochemical techniques, such as open circuit potential and potentiodynamic polarization measurements. The passive film formed on the surface was further confirmed by SEM and EDX.

2. Experimental

2.1. Materials and sample preparation

The weight loss and electrochemical experiments were performed on mild steel specimens having chemical compositions, C-0.16 %, Si-0.10 %, Mn-0.40 %, P-0.013%, S-0.02 %. The exposed dimensions were 3 cm × 1 cm × 0.1 cm and 1 cm² for the weight loss and electrochemical experiment, respectively. Before exposure to test solution, exposed areas were cleaned with different grades of emery paper, 1/0, 2/0, 3/0, and 4/0, washed with triple distilled water, degreased with absolute alcohol, and finally dried and stored in a desiccator. Specimens were weighed on an electronic balance (CONTECH, Model No.CBS-50, least count 0.001 g). 1 M HCl was prepared by diluting 36 % HCl (analytical grades) in double-distilled water for test solution.

2.2. Weight loss measurement

Due to the reliability and simplicity of the weight-loss method, it is preferably the starting method for corrosion testing. After initial weighing, the specimens were immersed in beakers that contained 100 mL of 1M HCl in the absence and presence of a different concentration of inhibitor at a temperature of 25±1 °C. After 24 h, the specimens were taken out, washed, dried, and weighed accurately. Mean corrosion rate (CR) in mg cm² h⁻¹ with respect to acid and inhibitor was calculated. The experiment was performed in triplicate to ensure reproducibility, and the mean value was reported. The corrosion rate (CR) was calculated from the following equation:

$$CR = \Delta W / At \quad (1)$$

Where CR is corrosion rate (mg cm⁻² h⁻¹), ΔW is the weight loss (mg), A is surface area (m²), and t is immersion time in h. The inhibition efficiency (% E) of inhibitor on the corrosion of mild steel was calculated as follows,

$$\%E = \frac{W_0 - W}{W_0} \times 100 \quad (2)$$

Where, W_0 and W are weights of mild steel in mg in the absence and presence of inhibitor, respectively.

2.3. Electrochemical measurement

Polarization studies were carried out using an electrochemical measurement system, DC 105, containing the DC corrosion technique from M/S Gamry instruments, 734 Louis

Drive, Warminster, PA, USA. For polarization studies, mild steel specimens having a surface area of 1cm^2 were exposed to the acid solution. Mild steel as working electrode, saturated calomel (SCE) as reference electrode, and graphite as the auxiliary electrode was used for all electrochemical measurements. Before each measurement, specimens were allowed to corrode freely for 1 h, and their OCPs were measured as a function of time to obtain a steady-state potential. The anodic and cathodic Tafel curves were obtained by changing the electrode potential automatically from -0.5 to 0.5 V at a scan rate of 5 mv/s polarization study was done with and without inhibitor in 1 M HCl.

2.4. Surface measurement

The surface film formed on the metal specimen was evaluated by SEM-EDAX analysis. This was carried out by SEM/EDAX model PHENOM PROX from the Netherlands. The spectra were recorded for specimens exposed to 1 M HCl for 24 h in the absence and presence of a 500 ppm inhibitor. The energy of the acceleration beam employed was 20 kV.

3. Results and Discussion

3.1. Weight loss experiment

The loss in the weight of mild steel coupons in 1 M HCl in the absence and presence of different concentrations of acetyl-1H-benzotriazole was determined after 24 h immersion period at 25 ± 1 °C. The percentage inhibition efficiency (% E) and degree of surface coverage (θ) were calculated and presented in Table 1.

Table 1. The weight loss parameter was obtained for mild steel in 1M HCl containing different concentrations of 1-acetyl-1H-benzotriazole.

Inhibitor	Concentration (ppm)	Weight loss (mg)	Corrosion rate ($\text{mgcm}^{-2}\text{h}^{-1}$)	surface coverage (θ)	(%) E
	0.00	235	32.638	---	---
1M HCl	100	122	16.944	0.480	48.00
	200	113	15.694	0.519	51.90
	300	78	10.833	0.668	66.80
ABTZ	400	63	8.750	0.732	73.20
	500	52	7.222	0.778	77.80

It can be observed from the table that the inhibition efficiency increased with an increase in the concentration of the inhibitor, and the compound acted as a good corrosion inhibitor for corrosion of mild steel in 1 M HCl. The parameter (θ) representing the part of the metal surface covered by the inhibitor's molecules increased as the inhibitor concentration increased.

3.2. Adsorption isotherm

Adsorption isotherms are often used to demonstrate the performance of organic adsorbent type inhibitors and are essential in determining the mechanisms of organic electrochemical reactions. The most frequently used adsorption isotherms are Langmuir, Temkin, and Frumkin isotherms, describing the relation between surface coverage θ and bulk concentration (C) [11]. The values of surface coverage θ were evaluated using the value of % IE, resulted from the weight loss experiment in 1M HCl. Fig. 1 shows a plot C/θ v/s C , gave a straight line with a regression coefficient (R^2) value very close to unity ($R^2=1$). It indicates that corrosion control takes place via adsorption. The adsorption of inhibitor molecules on mild steel surface obeys Langmuir adsorption isotherm. The equation can be represented as:

$$K_{\text{ads}} = \frac{\theta}{C(1-\theta)} \quad (3)$$

The equation can be rearranged to

$$C_{\text{inh}}/\theta = 1/K_{\text{ads}} + C_{\text{inh}} \quad (4)$$

Where, C_{inh} is the concentration of inhibitor, θ is surface coverage, and K_{ads} is the equilibrium constant for the adsorption-desorption process. The K_{ads} is related to standard free energy (ΔG_{ads}^0) of adsorption by the following relation.

$$(\Delta G_{\text{ads}}^0) = -2.303RT \log (55.5 K_{\text{ads}}) \quad (5)$$

Where R is the universal gas constant, T is the absolute temperature in K, and the numerical value 55.5 represents the molar concentration of water in acid solution.

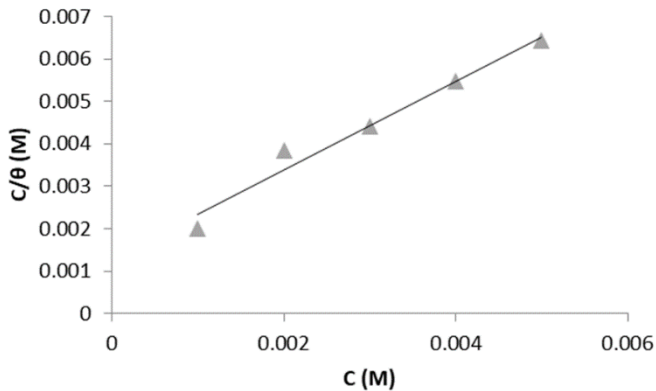


Fig. 1. Langmuir adsorption isotherm plot for the adsorption of 1-acetyl-1H-benzotriazole on mild steel surface in 1 M HCl solution.

Generally, the magnitude of ΔG_{ads} up to -20 kJ/mol is associated with physisorption, and those around -40 kJ/mol or more negatively associated with chemisorption. In the present case calculated value of ΔG_{ads} for the 1-acetyl-1H- benzotriazole was found to be -

27.07 KJ/mol. This indicated that the adsorption of inhibitors on the mild steel surface involved both physical and chemical processes [12-18].

4. Electrochemical Measurements

4.1. Open circuit potential (OCP) curves

The variation of open circuit potential with time for mild steel in 1M HCl solutions without and with acetyl-1H-benzotriazole is shown in Fig. 2. The plot shows an apparent change in the OCP curve due to the presence of the inhibitor. The curves shift in a positive direction in the presence of inhibitors. The inhibited solution exhibited a higher positive open circuit potential value when compared with those obtained in blank solution, indicating the formation of the protective film due to the adsorption of inhibitors on the mild steel surface. The continuous shift to the positive direction can be attributed to forming a protective and inhibitive film on a mild steel surface, increasing the inhibitor concentration and exposure period [19].

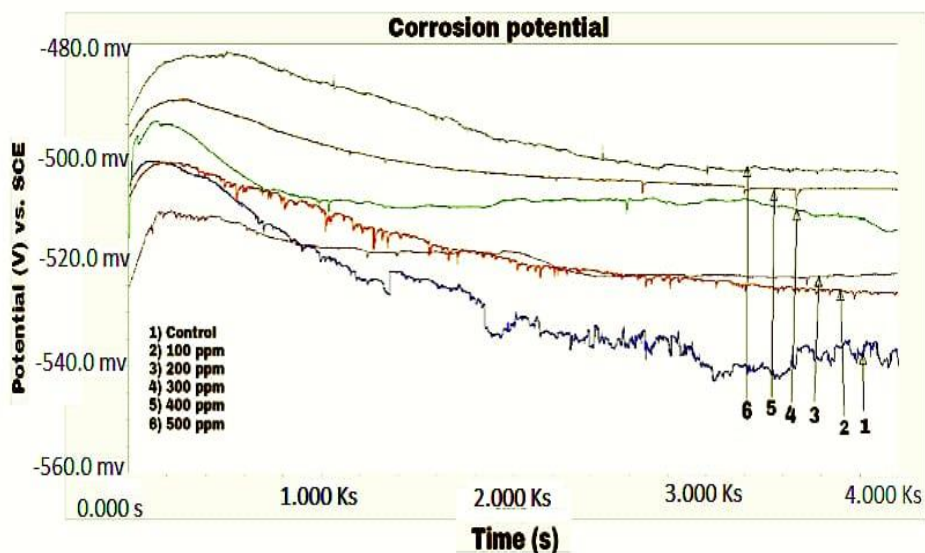


Fig. 2. Open circuit potential of mild steel without and with different concentrations of ABTZ inhibitor in 1M HCl.

4.2. Potentiodynamic polarisation studies

Polarization measurements were carried out in order to get information regarding the kinetics of anodic and cathodic reactions. The obtained polarization curves for mild steel in 1 M HCl in the absence and presence of a different concentration of 1-acetyl-1H-benzotriazole are shown in Fig. 3. Corrosion kinetic parameters E_{corr} , I_{corr} , Tafel (β_a , β_c),

and inhibition efficiency are depicted in Table 2. The corrosion inhibition efficiency was calculated by using the following equation:

$$\%IE = \frac{i_{corr,0} - i_{corr}}{i_{corr,0}} \times 100 \quad (6)$$

Where $i_{corr,0}$ and i_{corr} are the corrosion current densities in the absence and presence of inhibitor.

It is clear from Figures that both cathodic and anodic slopes shifted in a positive direction with the increase in inhibitor concentration. This could be attributed to the adsorption of inhibitors onto the metal surface [20-25].

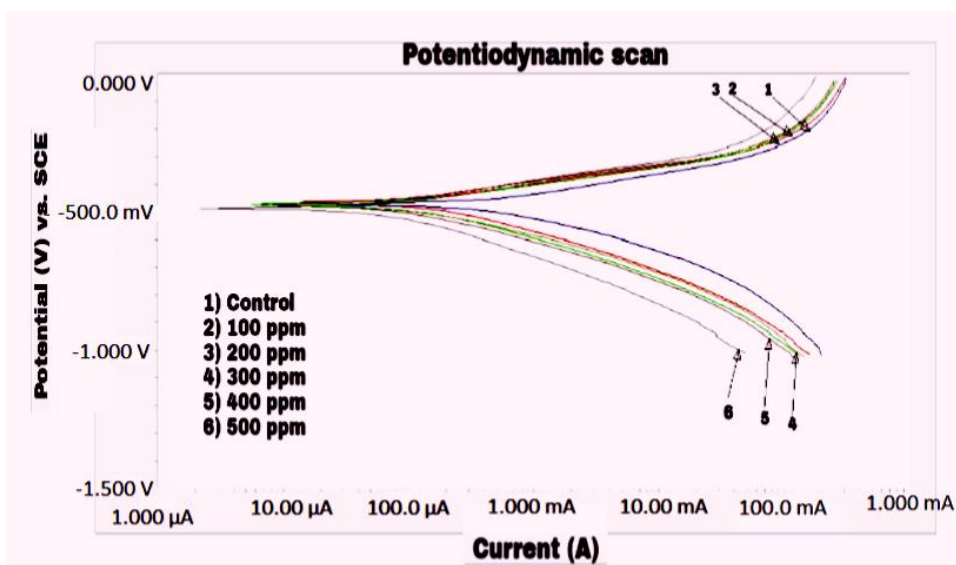


Fig. 3. Potentiodynamic polarization of mild steel without and with different concentrations of ABTZ in 1 M HCl.

The results reported in Table 2 indicate that the I_{corr} values decreased significantly with an increase in inhibitor concentration, and maximum inhibition efficiency of 80.55 % was obtained at 500 ppm concentration. This is due to the adsorption of inhibitors molecules onto the metal surface. Further, the concentration of inhibitor having less effect on corrosion potential (E_{corr}) suggest that the compound acted as mixed-type inhibitors and adsorbed on the surface, thereby blocking the corrosion reaction. As previously reported in the presence of inhibitor, if E_{corr} shift is greater than 85 mV with respect to E_{corr} in uninhibited solution, it can be considered cathodic or anodic type; otherwise, it is mixed. In the present study, the maximum deviation range was less than 85 mV, suggesting that ABTZ behaved as a mixed-type inhibitor [26-31].

Table 2. Tafel polarization parameters for mild steel in 1 M HCl in the absence and presence of a different concentration of ABTZ.

	Concentration of Inhibitors(ppm)	E_{corr} (mv)	I_{corr} ($\mu\text{A}/\text{cm}^2$)	β_a (v/dec)	β_c (v/dec)	% IE
	1 M HCl	-471.0	197.0	91.30×10^{-3}	163.4×10^{-3}	---
ABTZ	100	-494.0	104.0	77.20×10^{-3}	150.3×10^{-3}	47.20
	200	-491.0	92.19	90.13×10^{-3}	142.1×10^{-3}	53.20
	300	-488.0	62.84	59.34×10^{-3}	144.7×10^{-3}	68.10
	400	-485.0	52.30	74.33×10^{-3}	132.5×10^{-3}	73.45
	500	-487.0	38.30	53.67×10^{-3}	124.1×10^{-3}	80.55

5. Surface Studies

5.1. Scanning electron microscopic (SEM) analysis

A micrograph of the polished mild steel surface before immersion in 1 M HCl is shown in Fig. 4(a). The micrograph shows the presence of a smooth surface without pits. The micrograph of mild steel after immersion in 1 M HCl is shown in Fig. 4(b). The micrograph indicates that the surface was drastically damaged and corroded due to free acid attack in the absence of inhibitors. A micrograph of mild steel after immersion in 1M HCl solution containing 500 ppm of 1-acetyl-1H-benzotriazole is shown in Fig. 4(c). It was found that surface morphology is significantly improved due to the formation of protective film on the mild steel surface.

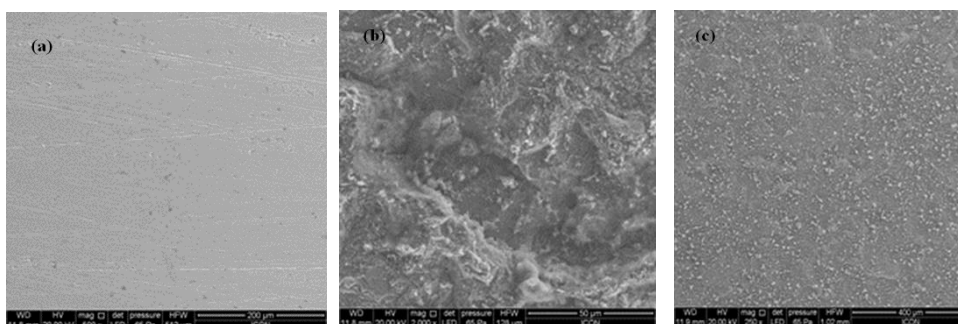


Fig. 4. SEM micrographs of mild steel surface (a) before immersion in 1 M HCl with the magnification of 500 x (b) after one-day immersion in 1M HCl with the magnification of 2000 x and (c) after one day of immersion in 1 M HCl+500 ppm of 1-acetyl-1H-benzotriazole with the magnification 250 x.

5.2. Energy-dispersive X-ray spectroscopy (EDAX)

Fig. 5 shows the spectral profile of mild steel specimens in the absence and presence of 1-acetyl-1H-benzotriazole. It is a graph of intensity versus energy in keV. The spectral profile of the polished mild steel specimen before immersion in 1M HCl shows the signal for Fe and O. After immersion in 1 M HCl, the spectral profile shows a signal for Fe

only as the signal for oxygen disappears due to the breaking of air formed oxide film. The spectral profiles in the presence of 1-acetyl-1H-benzotriazole shows additional peaks characteristic of N and O, indicating the adsorption of inhibitor molecule on the metal surface.

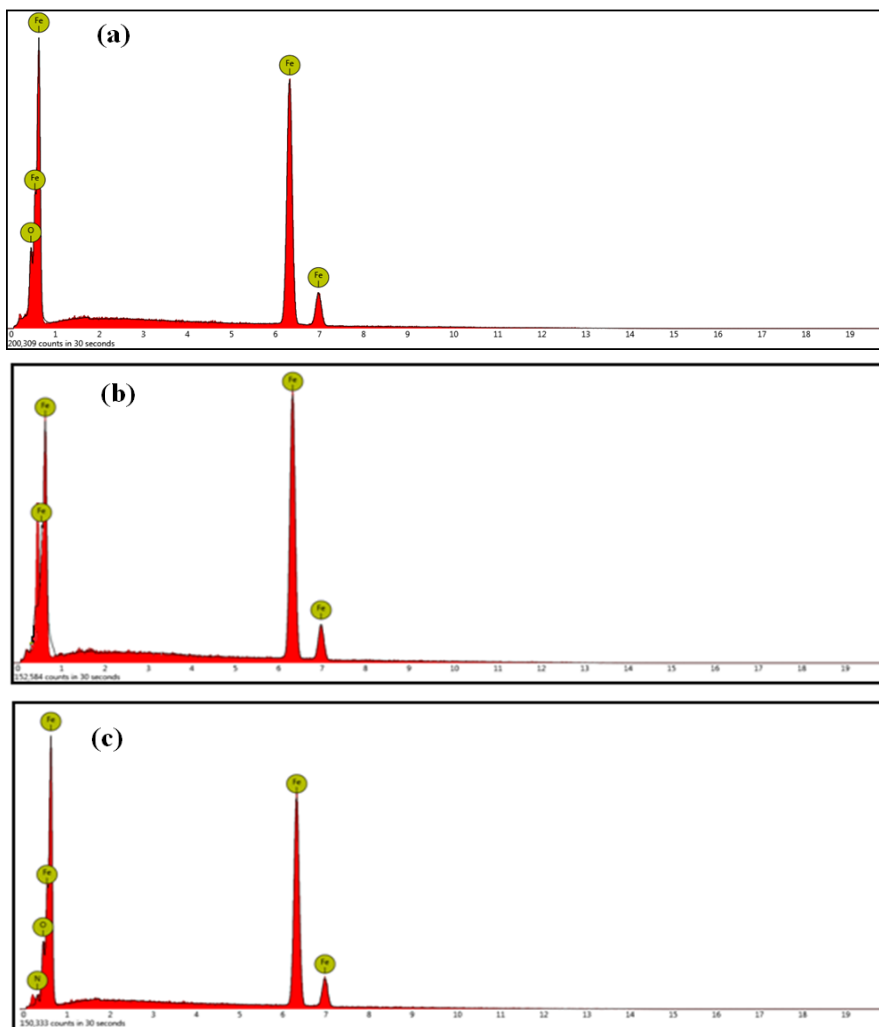


Fig. 5. EDX of mild surface (a) before immersion in 1 M HCl, (b) after one-day immersion in 1M HCl, and (c) after one day of immersion in 1 M HCl+500 ppm of 1-acetyl-1H-benzotriazole.

EDAX investigation thus confirmed the polarization data that inhibitor mitigated the corrosion of mild steel in 1 M HCl due to adsorption of its molecules on the mild steel surface, preventing it from being corroded easily.

6. Conclusion

The results proved that 1-acetyl-1H-benzotriazole displayed good corrosion inhibition for mild steel in 1M HCl solution. The inhibitor acted as a mixed type and shifted both cathodic and anodic curves in a positive direction. The percentage inhibition efficiency increased with an increase in the concentration of inhibitor. The data obtained from weight loss techniques fitted well into the Langmuir adsorption isotherm. SEM-EDX analysis showed an improvement in surface morphology of inhibited mild steel compared with uninhibited mild steel. So 1-acetyl-1H-benzotriazole was found to be a good inhibitor, as confirmed by all the chemical and electrochemical measurements.

Acknowledgments

This work was supported by the Department of Chemistry, R. J. College, University of Mumbai. The authors would like to acknowledge all the staff members for their support. The authors are also thankful to ICON Analytical Laboratory, Mumbai, for SEM and EDAX testing.

References

1. E. E. OGuzie, Y. Lie, and F. H. Wang, J. Coll. Interf. Sci. **310**, 90 (2007). <https://doi.org/10.1016/j.jcis.2007.01.038>
2. M. Seter, M. J. Thomson, J. Stoimenovski, D.R. Macfarlane, and M. Forsyth, Chem. Commun. **48**, 5983 (2012). <https://doi.org/10.1039/c2cc32375c>
3. D. Gopi, K. Govindraju, and L. Kavitha, J. Appl. Electrochem. **39**, 269 (2009). <https://doi.org/10.1007/s10800-008-9666-4>
4. A. M. Atta, G. A. El-Mahdy, H. A. Al-Lohedan, and A. R. O. Ezzat, Molecules **20**, 11131 (2015). <https://doi.org/10.3390/molecules200611131>
5. V. S. Sastry and J. R. Perumaredi, Corrosion **53**, 617 (1997). <https://doi.org/10.5006/1.3290294>
6. M. A. Migahed, E. M. S. Azzam, and A. M. Al. Sabagh, Mater. Chem. Phys. **85**, 273 (2004). <https://doi.org/10.1016/j.matchemphys.2003.12.027>
7. K. C. Emregal and O. Atakol, Mater. Chem. Phys. **82**, 188 (2003). [https://doi.org/10.1016/S0254-0584\(03\)00204-9](https://doi.org/10.1016/S0254-0584(03)00204-9)
8. F. Bentiss, M. Traisnel, H. Vezin, H. F. Hildebrand, and M. Lagrenee, Corros. Sci. **46**, 2781 (2004). <https://doi.org/10.1016/j.corsci.2004.04.001>
9. J. G. N. Thomas – *Proc. of 5th Eur. Symp. on Corrosion Inhibitors* (Ferrara, Italy, 1981) pp. 453.
10. N. Balamurugapandian, J. Sci. Res. **13**, 237(2021). <https://doi.org/10.3329/jsr.v13i1.48353>
11. E. S. H. E. Ashry, A. E. Nemr, S. A. Essawyand, and S. Ragab, ARKIVOC **11**, 205 (2006). <https://doi.org/10.3998/ark.5550190.0007.b21>
12. K. Fukui,. Theory of Orientation and Stereoselection (Springer-Verlag, New York, 1975). <https://doi.org/10.1002/qua.560110116>
13. M. Behpour, S. M. Ghoreishi, N. Soltani, M. Salavati-Niasari, M. Hamadani, and A. Gandomi, Corros. Sci. **50**, 2172 (2008). <https://doi.org/10.1016/j.corsci.2008.06.020>
14. I. B. Obot, N. O. Obi-Egbedi, and S. A. Umoren, Corros. Sci. **51**, 276 (2009). <https://doi.org/10.1016/j.corsci.2008.11.013>
15. E. A. Noor, Mater. Chem. Phys. **114**, 533 (2009). <https://doi.org/10.1016/j.matchemphys.2008.09.065>
16. G. Moretti, F. Guidi, and G. Grion, Corros. Sci. **46**, 387 (2004).

- [https://doi.org/10.1016/S0010-938X\(03\)00150-1](https://doi.org/10.1016/S0010-938X(03)00150-1)
17. M. A. Amin, S. S. A. El-Rehim, E. E. F. El-Sherbini, and R. S. Bayoumy, *Electrochim. Acta* **52**, 3588 (2007). <https://doi.org/10.1016/j.electacta.2006.10.019>
 18. X. Liu, P. C. Okafor, and Y. G. Zheng, *Corros. Sci.* **51**, 744 (2009). <https://doi.org/10.1016/j.corsci.2008.12.024>
 19. W. Yang, Q. Wang, K. Xu, and Y. Yin, *Material* **10**, 95 (2017).
 20. W. Villamizar, M. Casales, L. Martinez, J. G. Chacon-Naca, and J. G. Gonzalez-Rodriguez, *J. Solid State Electrochem.* **12**, 193 (2008). <https://doi.org/10.1007/s10008-007-0380-7>
 21. W. Villamizar, M. Casales, J. G. Gonzalez-Rodriguez, and L. Martinez, *J. Solid State Electrochem.* **11**, 619 (2007). <https://doi.org/10.1007/s10008-006-0208-x>
 22. W. Villamizar, M. Casales, J. G. Gonzales-Rodriguez, and L. Martinez, *Mater. Corros.* **57**, 696 (2006). <https://doi.org/10.1002/maco.200503957>
 23. L. M. Rivera-Grau, M. Casales, I. Regla, D. M. Ortega-Toledo, J. G. Gonzalez-Rodriguez, and L. Martinez-Gomez, *Int. J. Electrochem. Sci.* **7**, 13044 (2012).
 24. L. M. Rivera-Grau, M. Casales, I. Regla, D. M. Ortega-Toledo, J. A. Ascencio-Gutierrez, J. P. Calderon, and L. Martinez-Gomez, *Int. J. Electrochem. Sci.* **8**, 2491 (2013).
 25. X. Zhang, F. Wang, Y. He, and Y. Du, *Corros. Sci.* **43**, 1417 (2001). [https://doi.org/10.1016/S0010-938X\(00\)00160-8](https://doi.org/10.1016/S0010-938X(00)00160-8)
 26. F. Farelis and A. Ramirez, *Int. J. Electrochem. Sci.* **5**, 797 (2010).
 27. V. S. Saji, *Recent Patent Corros. Sci.* **1**, 63 (2011). <https://doi.org/10.2174/2210683911101010063>
 28. V. Jovancicevic, S. Ramachandran, and P. Prince, *Corrosion* **55**, 449 (1999). <https://doi.org/10.5006/1.3284006>
 29. C. Verma, M. Quraishi, and A. Singh, *J. Taibah University Sci.* **10**, 718 (2016). <https://doi.org/10.1016/j.jtusci.2015.10.005>
 30. M. Beytur, Z. Irak, S. Manap, and H. Yuksek, *Heliyon* **5**, ID e01809 (2019). <https://doi.org/10.1016/j.heliyon.2019.e01809>
 31. O. Akinbulumo, O. Odejebi, and E. Odekanle, *Results Mater.* **5**, ID 100074 (2020). <https://doi.org/10.1016/j.rinma.2020.100074>